Journal of Solid State Chemistry 184 (2011) 1850–1857

Contents lists available at ScienceDirect

Journal of Solid State Chemistry

journal homepage: www.elsevier.com/locate/jssc

Luminescent lanthanide complexes with 4-acetamidobenzoate: Synthesis, supramolecular assembly via hydrogen bonds, crystal structures and photoluminescence

Xia Yin, Jun Fan*, Zhi Hong Wang, Sheng Run Zheng, Jing Bo Tan, Wei Guang Zhang*

Institute of Special Materials & School of Chemistry and Environment, South China Normal University, Guangzhou 510006, PR China

ARTICLE INFO

Article history:
Received 9 March 2011
Received in revised form
3 May 2011
Accepted 15 May 2011
Available online 30 May 2011

Keywords:
Luminescent lanthanide complexes
4-Acetamidobenzoate
Supramolecular assembly
Photoluminescence

ABSTRACT

Four new luminescent complexes, namely, $[Eu(aba)_2(NO_3)(C_2H_5OH)_2]$ (**1**), $[Eu(aba)_3(H_2O)_2]\cdot 0.5$ (4, 4′-bpy)$\cdot 2H_2O$ (**2**), $[Eu_2(aba)_4(2, 2'\text{-bpy})_2(NO_3)_2]\cdot 4H_2O$ (**3**) and $[Tb_2(aba)_4(phen)_2(NO_3)_2]\cdot 2C_2H_5OH$ (**4**) were obtained by treating $Ln(NO_3)_3\cdot 6H_2O$ and 4-acetamidobenzoic acid (Haba) with different coligands (4, 4′-bpy=4, 4′–bipyridine, 2, 2′-bpy=2, 2′-bipyridine, and phen=1, 10-phenanthroline). They exhibit 1D chains (**1**–**2**) and dimeric structures (**3**–**4**), respectively. This structural variation is mainly attributed to the change of coligands and various coordination modes of aba molecules. Moreover, the coordination units are further connected via hydrogen bonds to form 2D even 3D supramolecular networks. These complexes show characteristic emissions in the visible region at room temperature. In addition, thermal behaviors of four complexes have been investigated under air atmosphere. The relationship between the structures and physical properties has been discussed.

1. Introduction

The development of luminescent probes and sensors based on lanthanide complexes [1–3] have gained great recognition in materials, biological and medical science over the past years, due to many advantages of f–f transitions in fluorescence spectra, such as extremely narrow emission profiles, large Stokes shifts and long fluorescence lifetimes [4,5]. These make luminescent materials including Ln(III) ions very attractive for a variety of applications, such as effective light conversion devices, fluorescent labels and probes for high sensitive time-resolved fluorimetric immunoassays [6–11]. Since the f–f transitions are parity-forbidden [4,5], free Ln(III) ions have low extinction coefficients leading to low luminescence intensity. It is well documented that sensitizers (chromophoric ligands), energy transfer from the sensitizers to the central ions, the types of solvent, coordination environment and spatial structures of the complexes have a significant influence on the emission characteristics of Ln(III) ions [12–16]. Especially, the design of multifunctional chromophoric ligands [9–11] has played a crucial role in the construction of lanthanide complexes with desirable luminescent properties.

Aromatic carboxylic acids and their derivates have multifunctional coordination sites with chelating and bridging ability and have been widely adopted to construct the fascinating network topologies in the field of crystal engineering [17–21]. In addition, chromophoric groups of these ligands can be able to absorb the photons provided by the light source and transfer it efficiently to the emitting levels of the Ln(III) ions. That is to say, these ligands can enhance the f–f electronic transitions through an intersystem energy transfer process. On the other hand, some aromatic diimines such as phen, 2, 2′-bpy and 4, 4′-bpy molecules may remarkably regulate structural topologies and fluorescent properties of resulting complexes [22–26]. 4-Acetamidobenzoic (Haba) (Scheme 1) attracted our attention due to two typical characteristics: (1) it contains only one carboxyl group, which is much easier to form complexes with lower dimension than multi-carboxylate ligands and may help us elucidate the relationship between the complexes' structures and physical properties; and (2) the acetamido group acts as a hydrogen bonding donor and an acceptor, which may facilitate the crystallization and result in diverse supramolecular networks. Herein, we introduce this ligand to synthesize four new luminescent complexes **1–4**. Synthesis, crystal structures and physical properties of these complexes will be presented in this work.

2. Experimental

2.1. Materials and physical measurements

4-Acetamidobenzoic acid (Haba) was prepared according to the literature [27]. Lanthanide nitrate hydrates were prepared by dissolving the respective oxides (99.5%) in 1:1 HNO_3 (v/v)

* Corresponding authors. Fax: +86 20 39310187.
E-mail addresses: fanj@scnu.edu.cn (J. Fan), wgzhang@scnu.edu.cn (W.G. Zhang).

0022-4596/$ - see front matter © 2011 Elsevier Inc. All rights reserved.
doi:10.1016/j.jssc.2011.05.018

followed by drying. All the other reagents were of analytical grade and used without any further purification. Elemental (C, H, N) analyses were preformed on a Thermo FlashEA112 elemental analyzer. IR spectra were recorded using Perkin–Elmer Spectrum One spectrometer with KBr pellets in the range 4000–400 cm^{-1}.

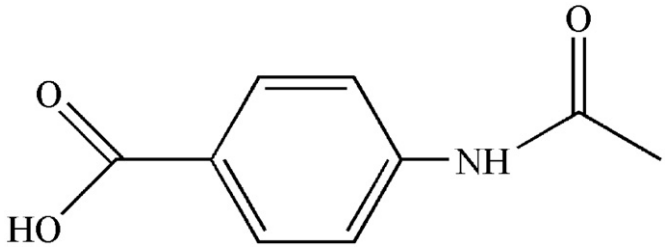

Scheme 1. Structure of Haba molecule.

X-ray powder diffraction measurements were carried out on a Bruker D8 Advance diffractometer at 40 kV, 40 mA with a Cu-target tube and a graphite monochromator. Thermogravimetric analysis (TGA) experiments were carried out on a Netzsch STA409PC Thermal Analyzer with a heating rate of 10 °C/min up to 800 °C under air atmosphere. Fluorescent spectra were measured with an Edinburgh FLS920 spectrophotometer at room temperature.

2.2. Syntheses of the complexes

2.2.1. Synthesis of $[Eu(aba)_2(NO_3)(C_2H_5OH)_2]$ (**1**)

A mixture of $Eu(NO_3)_3 \cdot 6H_2O$ (0.075 g, 0.017 mmol), Haba (0.090 g, 0.50 mmol) and triethylamine (0.10 mL) and ethanol (8 mL) was sealed in a 15 mL Teflon-lined stainless-steel reactor and then heated at 20 °C/h to 80 °C for 24 h under autogenous

Table 1
Crystallographic data and structure refinement summary for **1**–**4**.

Complex	**1**	**2**	**3**	**4**
Formula	$C_{22}H_{28}EuN_3O_{11}$	$C_{32}H_{36}EuN_4O_{13}$	$C_{56}H_{56}Eu_2N_{10}O_{22}$	$C_{64}H_{60}N_{10}O_{20}Tb_2$
Formula weight	662.43	836.61	1525.03	1607.06
Crystal system	Monoclinic	Triclinic	Triclinic	Triclinic
Space group	*C* 2/*c*	*P*−1	*P*−1	*P*−1
a (Å)	26.800(5)	9.4751(4)	10.176(2)	10.7612(2)
b (Å)	10.2651(19)	13.5774(5)	11.090(2)	11.1307(3)
c (Å)	9.6873(17)	14.8274(6)	14.294(3)	14.3438(3)
α (deg.)	90	94.650(2)	73.938(2)	76.7950(10)
β (deg.)	99.821(2)	90.727(3)	75.952(3)	74.5130(10)
γ (deg.)	90	109.247(2)	77.711(3)	82.090(2)
V (Å^3)	2626.0(8)	1793.38(12)	1485.3(5)	1606.55(6)
Z	4	2	1	1
D_c (g cm^{-3})	1.676	1.549	1.705	1.661
μ (mm^{-1})	2.450	1.817	2.181	2.267
F (0 0 0)	1328	846	764	804
Refl. measured	6615	20,638	7720	19,658
Unique refl. (R_{int})	2375 (0.0659)	6626 (0.0279)	5292 (0.0244)	5788 (0.0470)
GOF on F^2	1.036	1.122	0.989	1.004
Final *R* indices [$I > 2\sigma(I)$]	R_1=0.0456	R_1=0.0270	R_1=0.0448	R_1=0.0386
	wR_2=0.0784	wR_2=0.0615	wR_2=0.1113	wR_2=0.0884
R indices (all data)	R_1=0.0642	R_1=0.0315	R_1=0.0540	R_1=0.0468
	wR_2=0.0848	wR_2=0.0632	wR_2=0.1176	wR_2=0.0931

$R_1 = \sum ||F_o|-|F_c|| / \sum |F_o| \,.\, wR_2 = \{\sum [w(F_o^2-F_c^2]^2 / \sum [w(F_o^2)]^2\}^{1/2}$

Table 2
Selected bonds lengths (Å) for **1**–**4**.

Complex **1**					
Eu(1)−O(1)	2.283(5)	Eu(1)−O(4)	2.536(5)	Eu(1)−O(6)	2.457(4)
Eu(1)−O(1)$^{\#1}$	2.283(5)	Eu(1)−O(4)$^{\#1}$	2.536(5)	Eu(1)−O(6)$^{\#1}$	2.457(4)
Eu(1)−O(2)$^{\#2}$	2.312(5)	Eu(1)−O(2)$^{\#3}$	2.312(5)		
Complex **2**					
Eu(1)−O(1)	2.421(1)	Eu(1)−O(1w)	2.430(2)	Eu(1)−O(2w)	2.485(2)
Eu(1)−O(4)	2.581(2)	Eu(1)−O(5)	2.464(2)	Eu(1)−O(7)	2.325(2)
Eu(1)−O(8)$^{\#4}$	2.341(2)	Eu (1)−O(2)$^{\#5}$	2.3579(19)		
Complex **3**					
Eu(1)−O(1)	2.381(4)	Eu(1)−O(4)	2.425(4)	Eu(1)−O(5)	2.669(4)
Eu(1)−O(7)	2.556(4)	Eu(1)−O(8)	2.486(4)	Eu(1)−N(3)	2.631(5)
Eu(1)−N(4)	2.601(5)	Eu(1)−O(2)$^{\#6}$	2.363(4)	Eu(1)−O(5)$^{\#6}$	2.381(4)
Complex **4**					
Tb(1)−O(1)	2.321(3)	Tb(1)−O(4)	2.378(3)	Tb(1)−O(5)	2.685(3)
Tb(1)−O(7)	2.544(4)	Tb(1)−O(8)	2.438(4)	Tb(1)−N(3)	2.565(4)
Tb(1)−N(4)	2.607(4)	Tb(1)−O(2)$^{\#7}$	2.344(3)	Tb(1)−O(5)$^{\#7}$	2.337(3)

Symmetry transformations used to generate equivalent atoms: #1 $-x, y, 1/2-z$; #2 $-x, -y, -z$; #3 $x, -y, 1/2+z$; #4 $1-x, 1-y, -z$; #5 $2-x, 1-y, -z$; #6 $-x, 1-y, -z$; #7 $2-x, 1-y, 2-z$.

pressure. After slowly being cooled to room temperature at a rate of 5 °C/h, light-red block crystals of complex **1** were obtained with a yield of 55%. Calcd. for $C_{22}H_{28}EuN_3O_{11}$ (662.44): C 39.89, H 4.26, N 6.34; found: C 39.72, H 4.14, N 6.18%. IR (KBr, cm^{-1}): 3304 br, 1668 m, 1602 s, 1524 s, 1408 s, 1319 m, 1263 m, 1179 m, 1098 m, 862 w, 789 m.

2.2.2. Synthesis of $[Eu(aba)_3(H_2O)_2]\cdot 0.5$ (4, 4′-bpy)$\cdot 2H_2O$ (**2**)

A solution of $Eu(NO_3)_3\cdot 6\,H_2O$ (0.075 g, 0.017 mmol) in ethanol (5 mL) was added dropwise to a mixture solution of Haba (0.090 g, 0.50 mmol), 4, 4′-bipyridine (0.027 g, 0.17 mmol) and triethylamine (0.10 mL) in ethanol (10 mL). Then, the resulting mixture was stirred at room temperature for 1 h. Some colorless rod-like crystals of **2** were collected by slow evaporation of the solution for several weeks with 42% yield. Calcd for $C_{32}H_{36}EuN_4O_{13}$ (836.61): C 45.94, H 4.34, N 6.70; found: C 46.15, H 4.45, N 6.92%. IR (KBr, cm^{-1}): 3312 br, 1672 s, 1605 vs, 1520 s, 1418 vs, 1317 m, 1263 m, 1179 m, 864 m, 785 s.

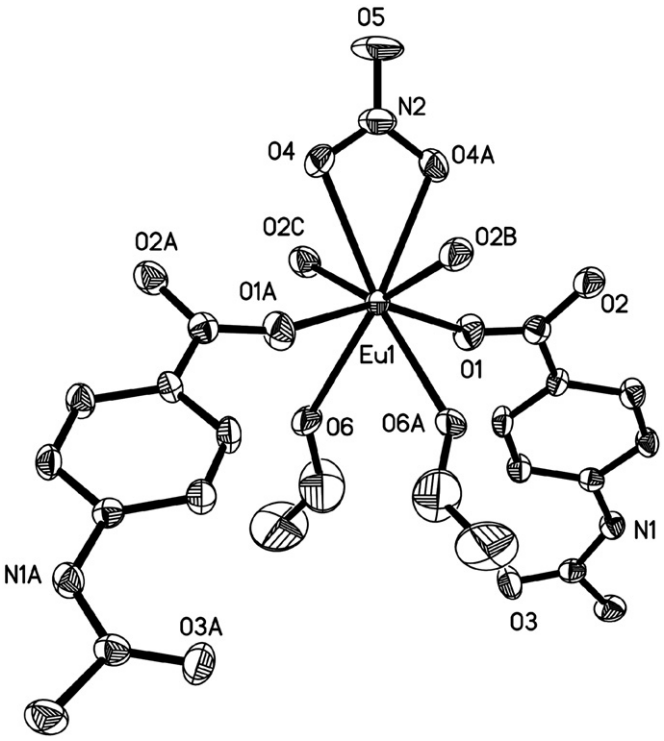

Fig. 1. ORTEP view of **1** with 30% thermal ellipsoids. All hydrogen atoms are omitted for clarity. Symmetry codes: A, $-x$, y, $1/2-z$; B, $-x$, $-y$, $-z$; C, x, $-y$, $1/2+z$.

2.2.3. Synthesis of $[Eu_2(aba)_4(2, 2'\text{-bpy})_2(NO_3)_2]\cdot 4\,H_2O$ (**3**)

Complex **3** was prepared in a similar procedure as that described in **2**, except that 2, 2′-bipyridine was replaced by 4, 4′-bipyridine. Some colorless block crystals of **3** were isolated by slow evaporation for several weeks with 48% yield. Calcd for $C_{56}H_{56}Eu_2N_{10}O_{22}$ (1525.03): C 44.10, H 3.70, N 9.18; found: C 44.28, H 3.75, N 9.32%. IR (KBr, cm^{-1}): 3266 br, 1675 m, 1604 vs, 1520 s, 1424 s, 1322 s, 1269 w, 1177 m, 1105 w, 1026 w, 864 m, 848 w, 787 m, 731 m.

2.2.4. Synthesis of $[Tb_2(aba)_4(phen)_2(NO_3)_2]\cdot 2C_2H_5OH$ (**4**)

A mixture of $Tb(NO_3)_3\cdot 6H_2O$ (0.077 g, 0.17 mmol), phen (0.034 g, 0.17 mmol), Haba (0.090 g, 0.50 mmol), triethylamine (0.1 mL) and ethanol (8 mL) was placed in a 15 mL Teflon-lined stainless-steel reactor and heated at 20 °C/h to 100 °C for 48 h under autogenous pressure. Colorless block crystals of compound **4** were obtained with a yield of 60%. Calcd for $C_{64}H_{60}Tb_2N_{10}O_{20}$ (1607.07): C 47.83, H 3.76, N 8.72; found: C 47.65, H 3.62, N 8.56%. IR (KBr, cm^{-1}): 3445 br, 1678 m, 1603 s, 1522 s, 1420 s, 1321 m, 1267 m, 1179 m, 1105 w, 864 w, 845 w, 787 m, 727 m.

2.3. X-ray crystallography

Diffraction data of compounds **1–4** were collected on a Bruker APEX II Smart CCD diffractometer equipped with graphite-monochromated Mo*K*α radiation (λ=0.71073 Å) using the ω-scan technique. Multi-scan absorption corrections were applied with the *SADABS* program [28]. The structures were solved by direct methods using the *SHELXS*-97 program and all the non-hydrogen atoms were refined anisotropically with the full-matrix least-squares on F^2 using the *SHELXL*-97 program [29]. The hydrogen atoms of water molecules were located in the difference Fourier maps and the other hydrogen atoms were generated

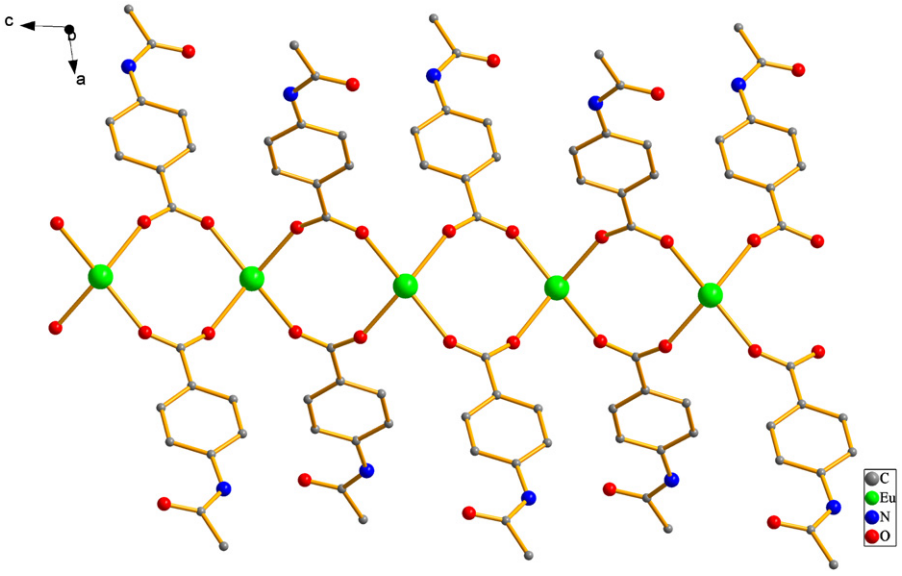

Fig. 2. Structural view of 1D chain in complex **1**. Chelate nitrates, ethanol molecules and all hydrogen atoms are omitted for clarity.

geometrically and refined as riding atoms with isotropic thermal factors. Crystallographic data and structure determination summaries for **1–4** are listed in Table 1 and the selected bond lengths are given in Table 2. The hydrogen bonds and selected bond angles for **1–4** are listed in Supporting Information, Tables S1 and S2, respectively. CCDC-794675 (**1**), 794676 (**2**), 794677 (**3**) and 794678 (**4**) contain the supplementary crystallographic data for this paper. Copies of these data can be obtained free of charge from The Cambridge Crystallographic Data Centre via www.ccdc.cam.ac.uk/ data_request/cif.

3. Results and discussion

3.1. Syntheses and IR spectra

In our previous studies [27], hydrothermal reactions of Ln(III) ions with Haba ligands and phen resulted in lanthanide complexes with mononuclear or dimeric structure features, which may be mainly ascribed to the lanthanide contraction effect. In this work, four new complexes **1–4** were obtained by treating the corresponding nitrates with Haba molecules and different coligands (4, 4′-bpy, 2, 2′-bpy and phen). These crystalline solids are stable in air, soluble in DMF and DMSO and sparingly soluble in water or common organic solvent such as ethanol, acetone and acetonitrile.

Their IR spectra show characteristic absorptions for the carboxylate stretching vibrations. The characteristic bands of carboxylate groups are shown in the range 1520–1678 cm^{-1} for asymmetric stretching (ν_{as}) and 1317–1424 cm^{-1} for symmetric stretching (ν_s) [30]. The absence of strong absorption peaks around 1710 cm^{-1} indicates that all carboxyl groups (−COOH) of Haba ligands are deprotonated. In addition, broad absorption bands observed in the range 3445–3266 cm^{-1} are ascribed to the ν_{O-H} stretching vibrations of water or ethanol molecules in these compounds [30].

3.2. Crystal structure descriptions

3.2.1. 1D chains of *1–2*

Complex **1** exhibits a 1D chain-like coordination polymer, crystallizing in a monoclinic fashion with space group *C*2/*c*. As illustrated in Fig. 1, each coordination unit consists of one Eu(III) ion, two aba ligands, one chelate nitrate and two ligated ethanol molecules. Each eight-coordinated Eu(III) ion exhibits a distorted dodecahedron coordination geometry. The distances of Eu–O bonds range from 2.284(5) to 2.536(5) Å, all of which are in accord with values previously reported for the Eu^{III} complexes [27, 31–33]. Further investigation indicates that adjacent Eu(III) ions are interconnected by the μ_2-bridging aba anions with the Eu…Eu separation of 4.966 Å, resulting in a 1D polymeric chain

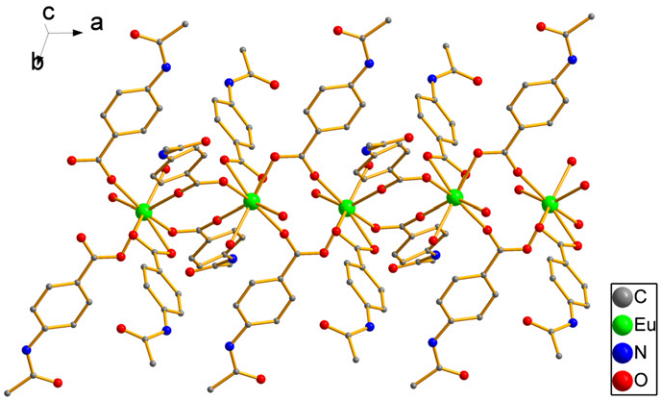

Fig. 4. Structural view of 1D chain in complex **2**. Lattice water molecules and all hydrogen atoms are omitted for clarity.

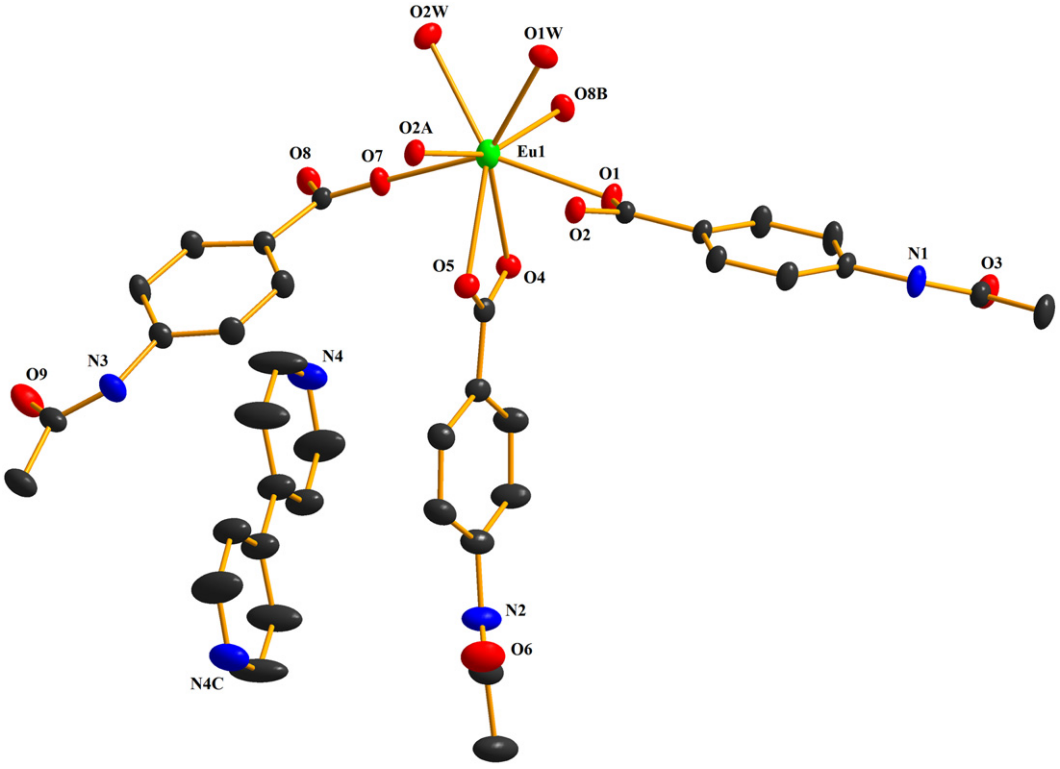

Fig. 3. Perspective view of the coordination environment of the Eu ions in complex **2** with atoms presented by 30% thermal ellipsoids (Hydrogen atoms are omitted for clarity). Symmetry codes: A, 1−*x*, 1−*y*, −*z*; B, 2−*x*, 1−*y*, −*z*; C, 1−*x*, 1−*y*, 1−*z*.

parallel to the *c*-axis (Fig. 2). In addition, there are N–H···O hydrogen bonds between acetamido groups of aba anions with carboxy oxygen atoms of adjacent ligands (N···O, 2.960 Å) (Table S1). Thus, adjacent 1D chains are linked by hydrogen bonds mentioned above to form an extended 2D supramolecular network with 1D tubular channels (Fig. S1). The coordinated ethanol molecules exist in these 1D channels.

X-ray crystallography reveals that complex **2** also displays a 1D chain consisting of $[Eu(aba)_3(H_2O)_2]$ building blocks, crystallizing in triclinic space group $P-1$. As shown in Fig. 3, the Eu(III) ion coordinates with six oxygen atoms from five aba anions and two ligated water molecules: eight oxygen atoms form a distorted dodecahedron configuration. The Eu–O bond distances are in the range from 2.324(2) to 2.582(2) Å, similar to those for the Eu(III) complexes [27, 31–33]. In the structure of **2**, the aba anions exhibit two kinds of coordination modes: one adopts chelating mode to bond with the Eu(III) ion; the others act as bidentate bridges to link adjacent Eu(III) ions with the Eu···Eu separation of 5.047 Å, forming a 1D chain along the *a*-axis (Fig. 4). Moreover, these adjacent chains are further extended through N–H···O hydrogen bonds between adjacent acetamido groups of aba anions (Table S1), thereby resulting in a 2D supramolecular network with 1D channel structures (Fig. S2). 4, 4′-bpy molecules are not engaged in coordinating with metal ions and occur in the 1D channels as guest molecules. The nitrogen atoms from the bpy molecules and the oxygen atoms (O1w) from the ligated water molecules also form N···H–O hydrogen bonds (N···O, 2.790 Å) (Table S1), thus greatly increasing the stabilities for the guest molecules in these channels.

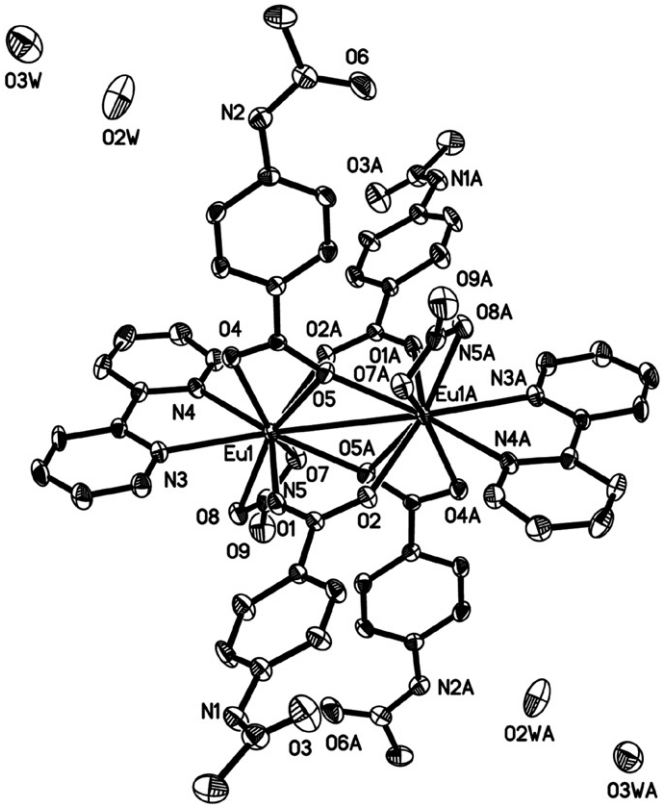

Fig. 5. ORTEP view of **3** with 30% thermal ellipsoids. All hydrogen atoms are omitted for clarity. Symmetry code: A, $-x$, $1-y$, $-z$.

3.2.2. *Dimeric structures of* ***3–4***

Compounds **3–4** possess similar dinuclear structures and both crystallize in the triclinic space group $P-1$, although having different metal atoms and different coligands.

In two compounds, the Ln(III) ions are nine-coordinated by five carboxylate oxygen atoms from four aba anions, two oxygen atoms from one nitrate and two nitrogen atoms from aromatic diimines [2, 2′-bpy (**3**) and phen (**4**), respectively] and both exhibit distorted tricapped trigonal prism coordination geometries [Fig. 5 (**3**) and Fig. S3 (**4**)]. The Ln–O and Ln–N bond lengths are within the normal ranges [27, 31–33]. The Eu···Eu separation in **3** is equal to 3.960(8) Å, while the corresponding Tb···Tb distance in **4** is 3.934(4) Å. These distances fall within the range of 3.785–4.532 Å that has observed for other Ln(III)-carboxylate complexes that feature both bidentate and tridentate bridging coordination modes [34]. Thus, two crystallographically equivalent Ln(III) ions are linked together through four bridging aba anions to form a dimeric unit. The free solvent molecules occupy in the lattice through hydrogen bonds (Table S1).

However, the connection of hydrogen bonds further results in different supramolecular frameworks.

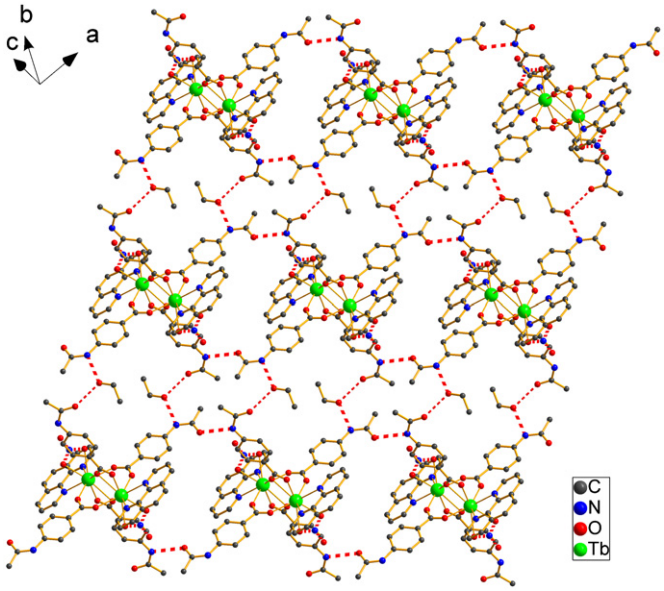

Fig. 7. A 2D layer structure linked by H-bonds in complex **4**.

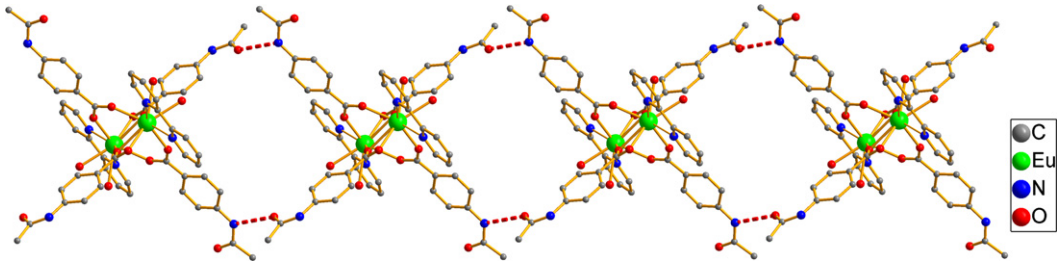

Fig. 6. View of 1D ring-like chain in complex **3** connected by hydrogen bonds.

In complex **3**, two acetamido groups of aba anions from two adjacent binuclear units form the intermolecular N–H···O hydrogen bonds (N···O, 2.880 Å) (Table S1) and the adjacent dimers are assembled to a 1D ring-like chain (Fig. 6). Moreover, the others hydrogen bonds (O–H···O and N–H···O, Table S1) between lattice water molecules and aba ligands further link these 1D chains to generate an extended 3D supramolecular structure (Fig. S4).

In complex **4**, uncoordinated acetamido groups of aba ligands act as not only the hydrogen bonding acceptors but also donors to form intermolecular N–H···O hydrogen bonds (N···O, 2.876 Å) (Table S1). In addition, ethanol molecules also take part in the formation of hydrogen bonds (N···O, 2.945 Å; O···O, 2.845 Å) (Table S1). Thus, the Tb(III) dinuclear units are extended through these H-bonds to form a 2D sheet-like network parallel to the *ac* plane (Fig. 7).

3.2.3. Structural comparison of complexes *1*–*4*

For four complexes in this work, X-ray crystallography reveals that they can be classified into two kinds of structure features: 1D chains (**1**–**2**) and binuclear structures (**3**–**4**). The possible explanation for this change might be the combination of the change of auxiliary ligands and the versatile coordination behavior of the aba anion.

As shown in Scheme 2, it is clearly demonstrated that the change of coligands greatly affected on their structures. For complex **1**, no aromatic imines are added into the reaction mixture and the aba ligands act as μ_2-bridges to connect adjacent Eu(III) ions, forming a 1D chain. In complex **2**, 4, 4′-bipyridine molecules do not coordinate to Eu(III) ions and exist in the lattice as guest molecules. A 1D chain is assembled through the coordination between the metal ions and the aba ligands. For **3**–**4**, aromatic diimines and nitrates adopt bidentate chelating modes to bind with Ln(III) ions and occupy four sites in the coordination spheres. The dimeric structure is further constructed through the connectivity of bridging aba ligands between two Ln(III) ions.

In addition, aba molecules exhibit coordination flexibility in these complexes: the carboxylate groups are coordinated to the Ln(III) ions in three different ways, namely, via chelating, bridging bidentate and tridentate [27]. Various coordination modes and connectivity are directly related to the resulting structure.

Furthermore, the extensive weak interactions have significant effect on the final packing. In these complexes, the acetamido groups of aba ligands act as the hydrogen bonding acceptors and donors to form the typical H-bonds with the other aba anions and solvent molecules, further generating the higher-dimensional supramolecular networks. In compounds **1**–**2**, 1D chains are extended to 2D supramolecular networks with 1D tubular channels. Ethanol and 4, 4′-bipyridine molecules exist in these channels, while intermolecular H-bonds link the Ln(III) dimers to form a 1D ring-like chain (**3**) and a 2D layer-like structure (**4**), respectively.

3.3. Powder XRD patterns

As illustrated in Fig. S5, X-ray powder diffraction profiles for complexes **1**–**4** are in agreement with those simulated on the basis of the single-crystal structures, respectively. The diffraction peaks on experimental patterns and simulated patterns correspond in the position, suggesting that the crystal samples are pure. The difference in reflection intensity between the simulated and experimental patterns is due to a certain degree of preferred orientation of the powder samples during data collection.

3.4. Thermal behaviors

From thermogravimetric analysis data for **1**–**4** (Fig. S6), each complex undergoes a mass loss in the first step (60–230 °C for **1**; below 200 °C for **2**–**4**), which corresponds to the removal of solvent and guest molecules (H_2O and C_2H_5OH). Subsequent thermal decompositions take place up to 650 °C, which may ascribe to the collapse of the coordination framework. Due to the existence of solvent molecules and possessing the low-dimensional coordination structures, four complexes do not exhibit high thermal stability. The detailed description for thermal analysis results is given in Supporting Information.

3.5. Luminescent properties

Due to the potential luminescent properties of Eu(III) and Tb(III) ions in the visible region, the luminescence investigations of compounds **1**–**3** were carried out in DMF solution (2.0×10^{-4} mol dm^{-3}) at room temperature.

Under the red emission of 616 nm, the excitation bands for Eu(III) complexes (**1**–**3**) exhibit similar peaks in the range from 370 to 410 nm and all the maximum excitation peaks are located around 395 nm (Fig. 8a). We further measured their corresponding emission spectra under the excited wavelength of 395 nm and they exhibit similar emission position except for different luminescent intensities. The emission spectra of three complexes (Fig. 8b) show the characteristic transition of $^5D_0 \rightarrow {}^7F_J$ (J=0–4) of Eu(III) ions in the range of 570–720 nm [31–33, 35], implying the ligand-to-europium energy transfer is efficient under the

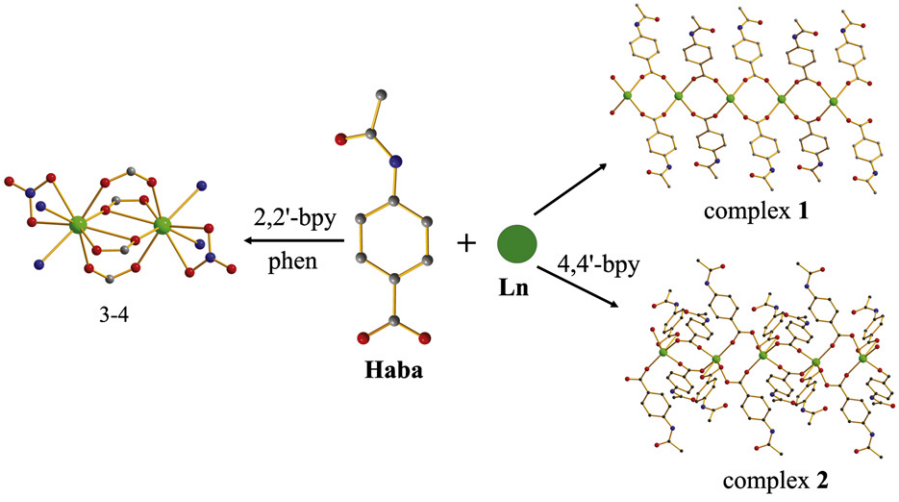

Scheme 2

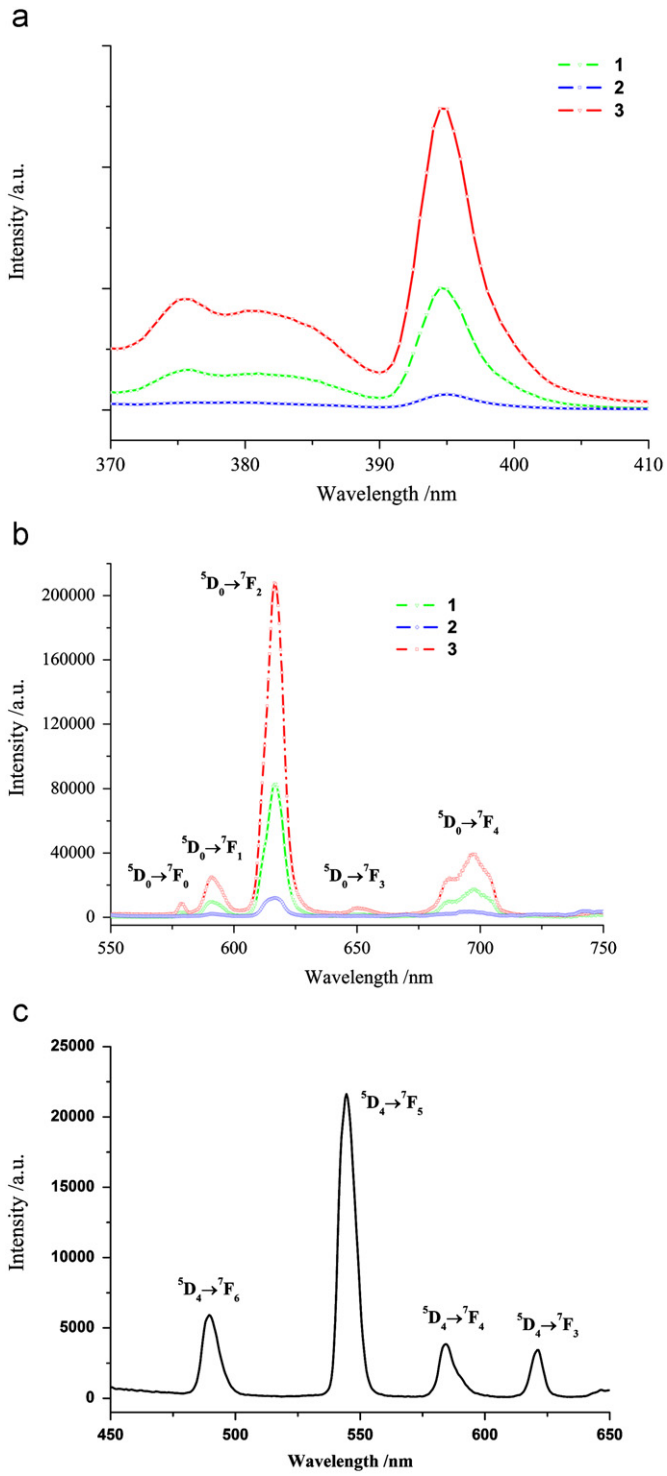

Fig. 8. (a) Excitation and (b) emission spectra of complexes **1–3** in DMF solution (2.0×10^{-4} mol dm^{-3}). (c) Emission spectra of complexes **4** (b, λ_{ex}=314 nm).

experimental conditions. The dominant band at ca. 616 nm is the hypersensitive $^5D_0\rightarrow{}^7F_2$ transition of Eu(III) ion, which is very sensitive to site symmetry and more intense than the $^5D_0\rightarrow{}^7F_1$ transition at about 590 nm. The intensity ratios I($^5D_0\rightarrow{}^7F_2$)/I($^5D_0\rightarrow{}^7F_1$) are equal to 8.40 for **1**, 1.36 for **2** and 8.45 for **3**, respectively, indicating the low symmetry site of the Eu(III) ions.

Compared with their emission spectra, the transition intensity changes in the order of **3** > **1** > **2** under the identical experimental conditions such as solvent, solution concentration, temperature, and slit widths etc, which indicates that the structures and coordination behavior of auxiliary ligands have clearly affected the emission behavior of the Eu(III) ion. In **1–3,** the coligands exist in the lattice as different forms. Complex **1** has no additional aromatic coligands. In the structure of **2**, 4, 4′-bpy molecule does not coordinate with the central ion and only occur as the guest. Two ligated water molecules occupy the coordination sphere. In complex **3**, 2, 2′-bpy molecules act as chelating ligands to take part in the coordination with Eu(III) ions. The aromatic groups of 2, 2′-bpy molecules can absorb the photons from the light source and transfer it efficiently to the emitting levels of the Eu (III) ions via Eu–N bonds. Thus, the f–f transition intensities can be enhanced through an efficient energy transfer process. At the same time, the metal ions are encapsulated by the organic ligands and the small solvent molecules do not enter the coordination sphere. Earlier results have indicated that the weak vibronic coupling between the Ln(III) ions and OH oscillators of solvent molecules provides a facile path for radiationless de-excitation of the metal ions [36]. On the basis of the reasons mentioned above, complex **3** shows stronger emissions in the visible region than complex **1–2**.

In addition, the solid samples **1–3** also exhibit strong, red emission under UV radiation and similar luminescent behaviors are observed at room temperature (Fig. S7).

The complex **4** emits an intense yellow–green light upon excitation of 314 nm and exhibits the characteristic transition of $^5D_4\rightarrow{}^7F_J$ (J=6−3) of the Tb(III) ions in the range of 470–640 nm (Fig. 8c), indicating that the organic ligands can transfer the energy effectively to the emitting levels of the Tb(III) ion under the experimental conditions [37]. Two intense emission bands at 487 and 544 nm correspond to $^5D_4\rightarrow{}^7F_6$ and $^5D_4\rightarrow{}^7F_5$, respectively, while the weaker emission bands at 586 and 622 nm originate from $^5D_4\rightarrow{}^7F_4$ and $^5D_4\rightarrow{}^7F_3$.

4. Conclusion

In summary, the reactions of Ln(III) ions with 4-acetamidobenzoate (aba) and different coligands resulted in four new luminescent complexes **1–4**. They exhibit two kinds of structural characteristics, such as 1D chains (**1–2**) and dimeric structures (**3–4**), attributed to the change of the coligands and various coordination modes of aba anions. In addition, they show strong, characteristic emission of Ln(III) ions in the visible region at room temperature and the results reveal that the types of auxiliary ligands and coordination structures of the complexes have significant effect on the construction of lanthanide complexes with desirable luminescent properties.

Acknowledgment

This work was granted financial support by the National Natural Science Foundation of China (No. 20771040), the Ministry of Science and Technology of China (No. 10C26214412704) and Guangdong Science and Technology Department (No. 2010B090300031).

Appendix A. Supplementary material

Supplementary data associated with this article can be found in the online version at doi:10.1016/j.jssc.2011.05.018.

References

[1] F.S. Richardson, Chem. Rev. 82 (1982) 541–552.
[2] Y. Kitamura, T. Ihara, Y. Tsujimura, Y. Osawa, D. Sasahara, M. Yamamoto, K. Okada, M. Tazaki, A. Jyo, J. Inorg. Biochem. 102 (2008) 1921–1931.

[3] P. Lenaerts, A. Storms, J. Mullens, J. D'Haen, C. Goerller-Walrand, K. Binnemans, K. Driesen, Chem. Mater. 17 (2005) 5194–5201.
[4] J.C.G. Bünzli, C. Piguet, Chem. Soc. Rev. 34 (2005) 1048–1077.
[5] J.C.G. Bünzli, in: J.C.G. Bünzli, G.R. Choppin (Eds.), Lanthanide Probes in life, chemical, and earth Sciences. Theory and Practice, Elsevier Scientific Publishers, Amsterdam, 1989 Chapter 7.
[6] N. Sabbatini, M. Guardigli, J.M. Lehn, Coord. Chem. Rev. 123 (1993) 201–228.
[7] C.H. Song, Z.Q. Ye, G.L. Wang, J.L. Yuan, Y.F. Guan, Chem. Eur. J. 16 (2010) 6464–6472.
[8] K. Hanaoka, K. Kikuchi, S. Kobayashi, T. Nagano, J. Am. Chem. Soc. 129 (2007) 13502–13509.
[9] J.P. Leonard, P. Jensen, T. McCabe, J.E. O'Brien, R.D. Peacock, P.E. Kruger, T. Gunnlaugsson, J. Am. Chem. Soc. 129 (2007) 10986–10987.
[10] S. Petoud, G. Muller, E.G. Moore, J.D. Xu, J. Sokolnicki, J.P. Riehl, U.N. Le, S.M. Cohen, K.N. Raymond, J. Am. Chem. Soc. 129 (2007) 77–83.
[11] G.F. De sa, O.L. Malta, C. De Mello Donega, A.M. Simas, R.L. Longo, P.A. Santa-Cruz, E.F. Da Silva Jr., Coord. Chem. Rev. 196 (2000) 165–195.
[12] Y.L. Guo, Y.W. Wang, W.S. Liu, W. Dou, X. Zhong, Spectrochimica Acta Part A 67 (2007) 624–627.
[13] S. Sivakumar, M.L.P. Reddy, A.H. Cowley, K.V. Vasudevan, Dalton Trans. 39 (2010) 776–786.
[14] C.M.G. dos Santos, A.J. Harte, S.J. Quinn, T. Gunnlaugsson, Coord. Chem. Rev. 252 (2008) 2512–2527.
[15] P. Mahata, K.V. Ramya, S. Natarajan, Chem.-Eur. J. 14 (2008) 5839–5840.
[16] D. Bradshaw, J.B. Claridge, E.J. Cussen, T.J. Prior, M.J. Rosseinsky, Acc. Chem. Res. 38 (2005) 273–282.
[17] Y. Huang, B. Yan, M. Shao, J. Solid State Chem. 182 (2009) 657–668.
[18] M.S. Liu, Q.Y. Yu, Y.P. Cai, C.Y. Su, X.M. Lin, X.X. Zhou, J.W. Cai, Cryst. Growth Des. 8 (2008) 4083–4091.
[19] Y.C. Qiu, Z.H. Liu, J.X. Mou, H. Deng, M. Zeller, Cryst. Eng. Commun. 12 (2010) 277–290.
[20] Y.J. Zhu, Z.G. Ren, W.H. Zhang, Y. Chen, H.X. Li, Y. Zhang, J.P. Lang, Inorg. Chem. Commun. 10 (2007) 485–488.
[21] Y.Q. Sun, J. Zhang, Y.M. Chen, G.Y. Yang, Angew. Chem. Int. Ed. 44 (2005) 5814–5817.
[22] H.M. Ye, N. Ren, J.J. Zhang, S.J. Sun, J.F. Wang, New J. Chem. 34 (2010) 533–540.
[23] L.N. Sun, Y. Zhang, J.B. Yu, C.Y. Peng, H.J. Zhang, J. Photochem. Photobio. A 199 (2008) 57–63.
[24] L. Bertolo, S. Tamburini, P.A. Vigato, W. Porzio, G. Macchi, F. Meinardi, Eur. J. Inorg. Chem. (2006) 2370.
[25] Q.B. Bo, Z.X. Sun, W. Forsling, Cryst. Eng. Commun. 10 (2008) 232–238.
[26] D. Guo, C.Y. Duan, F. Lu, Y. Hasegawa, Q.J. Meng, S. Yanagid, Chem. Commun. (2004) 1486–1487.
[27] Z.H. Wang, J. Fan, W.G. Zhang, Z. Anorg. Allg. Chem. 635 (2009) 2333–2339.
[28] Smart, Bruker, Saint, Bruker AXS Inc.: Madison, Wisconsin, 2004.
[29] G.M. Sheldrick, SHELXS-97 and SHELXL-97, University of Göttingen, Germany, 1997.
[30] K. Nakamoto, Infrared and Raman Spectra of Inorganic and Coordination Compounds, 5th ed., Wiley & Sons, New York, 1997.
[31] J. Fan, Z.H. Wang, M. Yang, X. Yin, W.G. Zhang, Z.F. Huang, R.H. Zeng, Cryst. Eng. Commun. 12 (2010) 216–225.
[32] J. Wang, J. Fan, L.Y. Guo, X. Yin, Z.H. Wang, W.G. Zhang, J. Solid State Chem. 183 (2010) 575–583.
[33] L. Cañadillas-Delgado, O. Fabelo, J. Pasán, F.S. Delgado, M. Déniz, E. Sepúlveda, M.M. Laz, M. Julve, C. Ruiz-Pérez, Cryst. Growth Des. 8 (2008) 1313–1318.
[34] A.R. Ramya, M.L.P. Reddy, A.H. Cowley, K.V. Vasudevan, Inorg. Chem. 49 (2010) 2407–2415.
[35] X.F. Li, Z.L. Xie, J.X. Lin, R. Cao, J. Solid. State Chem. 182 (2009) 2290–2297.
[36] M. Latva, H. Takalo, V.M. Mukkala, C. Matachescu, J.C. Rodríguez-Ubis, J. Kankare, J. Lumin. 75 (1997) 149–169.
[37] J.W. Cheng, S.T. Zheng, G.Y. Yang, Dalton Trans. (2007) 4059–4066.